Tuning the polarization and magnetism in $BiCoO_3$ by strain and oxygen vacancy effect: A first-principle study

Xing-Yuan Chen,[1] Li-Juan Chen,[1] Xiao-Bao Yang,[1] Yu-Jun Zhao,[1,a)] Hang-Chen Ding,[2] and Chun-Gang Duan[2]
[1]*Department of Physics and State Key Laboratory of Luminescent Materials and Devices, South China University of Technology, Guangzhou 510640, People's Republic of China,*
[2]*Key Laboratory of Polar Materials and Devices, Ministry of Education, East China Normal University, Shanghai 200241, China*

(Received 3 August 2011; accepted 30 November 2011; published online 3 January 2012)

The tensile strain and oxygen vacancy effects on the electronic and magnetic properties of multiferroic material $BiCoO_3$ have been studied by density functional theory + U calculations. It is found that the oxygen vacancy at the top of the pyramid structure along the ⟨001⟩ direction (denoted as O1) can be stabilized at 1+ and 2+ charge states, which significantly changes the local magnetic moment of Co ions and possibly provides net magnetic moments to the $BiCoO_3$ system. While the tensile strain degrades the polarization of $BiCoO_3$ about 20 $\mu C/cm^2$, the formation of oxygen vacancies becomes easier as the strain increases up to 5%. It indicates that the polarization and magnetic property of $BiCoO_3$ could be tuned by the strain and oxygen vacancies, though the polarization of $BiCoO_3$ is slightly degraded by the oxygen vacancies. Meanwhile, the change of electronic structure and magnetic property introduced by oxygen vacancy is illustrated according to the crystal field theory. © *2012 American Institute of Physics*. [doi:10.1063/1.3672837]

I. INTRODUCTION

$BiCoO_3$ has attracted intensive interest by many research groups as a new type of multiferroic materials,[1–7] which possess rich physics and great hope in magnetoelectronic applications. The crystal and magnetic structures of $BiCoO_3$ were studied by the Rietveld method from neutron diffraction data measured at temperatures from 5 to 520 K.[2] Since then, the electronic and magnetic properties of $BiCoO_3$ have also been investigated by *ab initio* density-functional calculations.[3] Both the experimental and theoretical studies have shown that the C-type antiferromagnetic (C-AFM) configuration is favored for the most stable tetragonal structure of $BiCoO_3$, which has a large c/a value (1.27).[2,3]

High magnetoelectric response and possible ferromagnetism are critical for the application of multiferroic magnetoelectric materials and thus have been a focus on the study of $BiCoO_3$ nowadays. The high pressure effect on $BiCoO_3$ was studied by first–principles calculations, and it was reported that no tetragonal-to-cubic or ferroelectric-to-paraelectric phase transition occurred up to 30 GPa, but the local magnetic moment of Co collapses at 4 GPa coupled with an insulator-to-semimetal transition.[5] A high spin to low spin transition of Co^{3+} ions at high pressures was reported to be responsible for the local moment collapse.[7] Consequently, a large magnetoelectric coupling was reported in $BiCoO_3$, as an external electric field could induce a transition of Co from high spin to low spin to realize the magnetic property manipulation by electric field.[4] Our recent work also showed that a possible ferrimagnetism in $BiCoO_3$ could be realized by Fe, Cr doping at the Co site.[8]

Meanwhile, more and more studies have discovered that strains and oxygen vacancies hold a remarkable influence on the magnetic and polarization properties of the perovskite materials, such as $SrTiO_3$,[9] $BiMnO_3$,[10] $SrMnO_3$,[11] and $BiFeO_3$.[12–18] A recent review about the strain effect on ferroelectric thin film can be found in Ref. 19. Strain and vacancy effects on $BiFeO_3$ have been regarded as being responsible for its high Curie temperature.[20] Epitaxial strain can influence the ferroelectric polarization and the Curie temperature dramatically in $BiFeO_3$.[18] Oxygen vacancies can lead to a transition of oxidation state of Fe from 3+ to 2+ and a noticeable change of its total magnetic moment in $BiFeO_3$.[12] It was reported that the optical conductivity could also be significantly influenced by oxygen vacancies, since the absorption edge shifts to a lower energy with the increase of oxygen vacancy concentration without the change of the main absorption peak.[13,14] Lately, Lee and Rabe reported that epitaxial strains may drive $SrMnO_3$ from the antiferromagnetic-paraelectric ground state to an unreported multiferroic ferroelectric-ferromagnetic state.[11] To our best knowledge, however, no strain and oxygen vacancy effects were investigated on the $BiCoO_3$ system, though a large magnetoelectric coupling and potential applications had been predicted in $BiCoO_3$.[4]

In this work, we studied the influence of strain and various oxygen vacancies with possible charge states on the multiferroic property of $BiCoO_3$. We found that the ferroelectric polarization decreases by ~10% as the tensile epitaxial strain increases up to 5%. While the strain has little influence on the magnetic property, oxygen vacancies change the local magnetic moments of $BiCoO_3$ and possibly provide remnant

a)Author to whom correspondence should be addressed. Electronic mail: zhaoyj@scut.edu.cn.

magnetic moments in addition to a slight reduction of the ferroelectric polarization. Furthermore, the magnetic property introduced by the oxygen vacancies are explained by a simple picture based on crystal field theory.

II. COMPUTATIONAL METHOD

To simulate the strain and oxygen vacancy effect, a $2 \times 2 \times 2$ super cell of $BiCoO_3$ containing 40 atoms was employed (c.f. Fig. 1). There are two types of nonequivalent oxygen ions in the cell: those at the top of the pyramid structure along the $\langle 001 \rangle$ direction are denoted as O1 and the other nonequivalent O ions are denoted as O2. The detailed calculations were carried out by a plane wave method with the interactions between valence electrons and ions represented by the projector augmented wave (PAW) pseudopotentials, as implemented in the Vienna *ab-initio* simulation package (VASP).[21,22] The generalized gradient approximation (GGA) of PW91 functional was employed for the exchange and correlation potential.[23,24] In order to get a better description of the electronic structure of $BiCoO_3$, all the calculations throughout this work were based on the GGA + U approach with an additional term of Hubbard model strong Coulomb correlation to the Co 3*d* electrons.[25] $U = 3$ eV and $J = 0$ eV, i.e., effective $U_{\text{eff}} = U - J = 3$ eV, were adopted in the GGA + U calculations based on the adjustment of local magnetic moments of $BiCoO_3$ to be in line with the experiment values.[2] The radii of Bi, Co, and O were set to 1.635, 1.302, and 0.802 Å, respectively, for the calculations of local magnetic moment and projected density of states (DOS). The energy cutoff was set to 500 eV, and a $5 \times 5 \times 5$ Monkhorst-Pack grid[26] was used for the $2 \times 2 \times 2$ super cell model. The lattice vectors and the ionic positions were fully relaxed until the Hellman-Feynman forces were less than 0.01 eV/Å.

Vacancies at both oxygen lattice sites were taken into account with the consideration of possible charge states of $q = 0, +1,$ and $+2$. Here, the image charge correction[27] (typically within 200 meV) was not employed, which is not expected to affect our conclusion. Ferroelectric polarization is studied by the modern polarization theory of Berry phase method.[28,29]

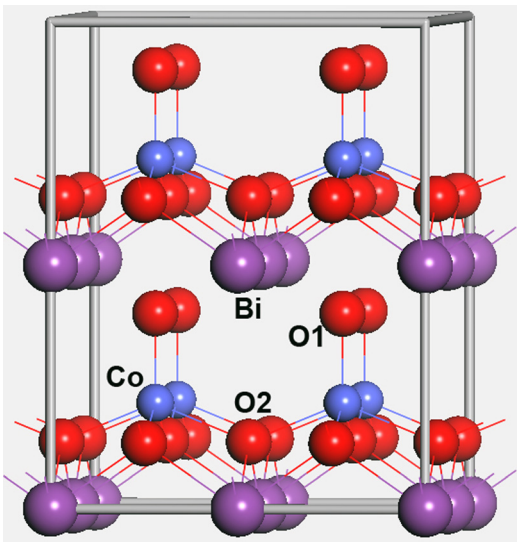

FIG. 1. (Color online) The $2 \times 2 \times 2$ $BiCoO_3$ superlattice with the bismuth (purple), cobalt (blue), and two nonequivalent oxygen atoms (red), marked as Bi, Co, O1, and O2.

III. RESULTS AND DISCUSSION

A. Strain effect in $BiCoO_3$

The tetragonal $BiCoO_3$ thin film may be grown on various substrates with remarkable lattice mismatch to $BiCoO_3$. The practical substrate lattice parameters are typically greater than 3.72 Å ($BiCoO_3$), such as 3.79 Å ($LaAlO_3$), 3.89 Å ($SrTiO_3$), 3.94 Å ($DyScO_3$), etc.[30–33] Therefore, epitaxial tensile strains were introduced here by increasing the $BiCoO_3$ lattice parameter of (*a, b*) plane by 1% to 5%, with the corresponding lattice parameter *c* relaxed to simulate the tetragonal $BiCoO_3$ thin films.

The changes of calculated polarization of $BiCoO_3$ with respect to the tensile strain are shown in Fig. 2, as well as the changes of *c*/*a* values and cell volumes. It is clear that the tensile strain on the (*a,b*) plane leads to a greater cell volume and a reduced *c*/*a* ratio. When the tensile strain is up to 5%, the cell volume has expanded by 6.3%. The calculated polarization value of 174.5 $\mu C/cm^2$ for $BiCoO_3$ at zero strain is consistent with earlier reports.[1,4] The calculated ferroelectric polarization showed a linear decrease to 156.3 $\mu C/cm^2$ along the z direction as the strain increases to 5%. In contrast, the tensile strain on the monoclinic or rhombohedral R3c structure $BiFeO_3$ can introduce additional out-of-plane polarization, though the ferroelectric polarization of tetragonal $BiFeO_3$ was reported to keep at about 150 $\mu C/cm^2$ with strains.[17] Different from the monoclinic or rhombohedra R3c structure in $BiFeO_3$, $BiCoO_3$ was reported to be with a tetragonal structure in most experiments.[2,7] Thus, it was supposed to keep its tetragonal structure with *P4mn* space group in our simulations, showing polarization along (001) only, without in-plane polarization due to the symmetry restriction.

The overall reduction of the polarization of $BiCoO_3$ induced by the tensile strain is also reflected from the Born effective charges[34] of Bi, Co, and O (c.f. Table I), along with

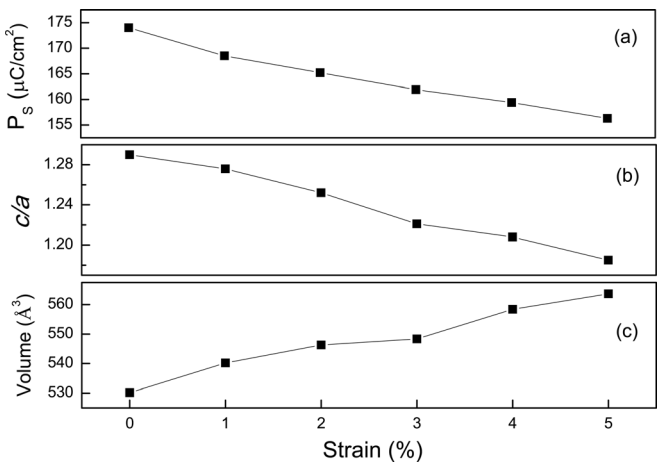

FIG. 2. The polarization value (a), *c*/*a* (b), and volumes (c) of pure $BiCoO_3$ under epitaxial strains from 0 to 5%.

TABLE I. The Born effective charges (BEC) of Bi, Co, and O under various tensile strains.

Strain	Bi	Co	O1	O2
0%	4.11	3.19	–3.36	–2.13
1%	3.96	3.28	–3.21	–2.00
2%	3.84	3.27	–3.15	–1.99
3%	3.65	3.3	–2.97	–1.86
4%	3.57	3.16	–2.9	–1.83
5%	3.40	3.14	–2.93	–1.81

the expanding volume and decreasing c/a value (c.f. Fig. 2). The magnitude of Born effective charges of Bi, Co, and O decreases slightly, in general, and the volume of $BiCoO_3$ expands almost linearly as the tensile strain increases, coupled with the decreasing c/a value.

The local magnetic moments of $BiCoO_3$ are mostly located at Co (2.85 μ_B) and O1 (0.36 μ_B) ions, which are merely changed to 2.86 and 0.41 μ_B, respectively, when 5% tensile strain is applied. This indicates that the local magnetic properties are hardly affected by the tensile strains.

B. The stability of oxygen vacancies

Oxygen vacancy often plays important roles in the magnetic and electronic properties of metal oxides. Here, the stable chemical potential region of $BiCoO_3$ with respect to its competition phases (such as Bi_2O_3, CoO, Co_3O_4, etc.) were investigated before the discussion of oxygen vacancy stability, which strongly depends on the preparation condition of samples.

In order to avoid precipitation of solid elemental crystals, the atomic potentials should be smaller than those in their corresponding elemental solids. That is,

$$\Delta\mu_{\mathrm{Bi}} \leq 0, \quad \Delta\mu_{\mathrm{Co}} \leq 0, \quad \text{and} \quad \Delta\mu_{\mathrm{O}} \leq 0. \tag{1}$$

The sum of $BiCoO_3$ atomic chemical potentials should be determined by the formation enthalpy of $BiCoO_3$ under equilibrium condition,

$$\Delta\mu_{\mathrm{Bi}} + \Delta\mu_{\mathrm{Co}} + 3\Delta\mu_{\mathrm{O}} = \Delta\mathrm{H}(\mathrm{BiCoO_3}). \tag{2}$$

$\Delta\mathrm{H}(\mathrm{BiCoO_3})$ denotes the formation enthalpy of $BiCoO_3$. Furthermore, the chemical potentials of Bi, Co, and O atoms also should be restricted by their corresponding competition phases,

$$\begin{aligned} 2\Delta\mu_{\mathrm{Bi}} + 3\Delta\mu_{\mathrm{O}} &\leq \Delta\mathrm{H}(\mathrm{Bi_2O_3}), \\ \Delta\mu_{\mathrm{Co}} + \Delta\mu_{\mathrm{O}} &\leq \Delta\mathrm{H}(\mathrm{CoO}), \\ 3\Delta\mu_{\mathrm{Co}} + 4\Delta\mu_{\mathrm{O}} &\leq \Delta\mathrm{H}(\mathrm{Co_3O_4}). \end{aligned} \tag{3}$$

The range of $\Delta\mu_{\mathrm{Bi}}$, $\Delta\mu_{\mathrm{Co}}$, and $\Delta\mu_{\mathrm{Co}}$ is determined by Eq. (2) and inequalities in Eq. (1) and (3), as shown in Fig. 3. The stable chemical potential region of $BiCoO_3$ is limited in the quadrangle ABCD and, thus, the chemical potential of oxygen can be tuned in the range of –1.319 to 0 eV. $BiCoO_3$ is easier to be synthesized under oxygen-rich conditions, while

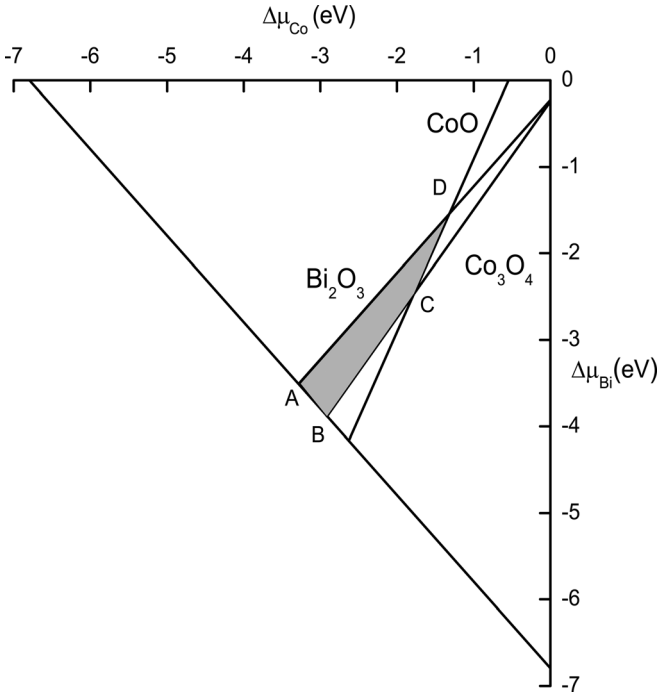

FIG. 3. GGA + U calculated stable chemical potential region (ABCD) for $BiCoO_3$.

the CoO and Bi_2O_3 phases prevail under oxygen poor conditions.

In semiconductors and insulators, the charge state of a defect could be changed as the Fermi level adjusted with the dominant defects in the sample.[35,36] Here, the most stable charge state of the oxygen vacancy defects is also discussed before we study the impact of defects on the multiferroic property. It is known that O vacancies could exist in three possible charge states (q = 0, 1+, and 2+), all of which were considered at both nonequivalent oxygen sites, O1 and O2, in $BiCoO_3$. The stability of oxygen vacancies at various charge states can be determined by their defect formation energies, depending on the chemical potential of oxygen and the Fermi energy,[37]

$$\begin{aligned} \Delta H_f^{(\alpha,q)} = E(\alpha,q) - E(0) + \sum_{\alpha} n_\alpha(\mu_\alpha + \triangle\mu_\alpha) \\ + q(E_{\mathrm{VBM}} + E_{\mathrm{F}}), \end{aligned} \tag{4}$$

where $E(\alpha,q)$ stands for the total energy of the super cell with O vacancy at a charge state of q. $E(0)$ is the total energy of perfect super cell, and E_{VBM} represents the energy of the VBM of the defect-free system. The oxygen chemical potential μ_α is referred to that of the O_2 molecule. $\triangle\mu_\alpha$ is the relative oxygen molecule chemical potential, and n_α is the number of vacancy atoms.

The calculated defect formation energies of oxygen vacancies with respect to the Fermi level are shown in Fig. 4. It indicates that O1 vacancy could be stabilized at charge states of 1+ and 2+, while the O2 vacancy of neutral charge state will be more stable than O1 vacancy at the Fermi levels close to the conduction-band minimum (CBM). Without the tensile strain, it takes at least 1 eV to form an oxygen vacancy defect under the oxygen-rich condition (see V_{O1}^{2+} in

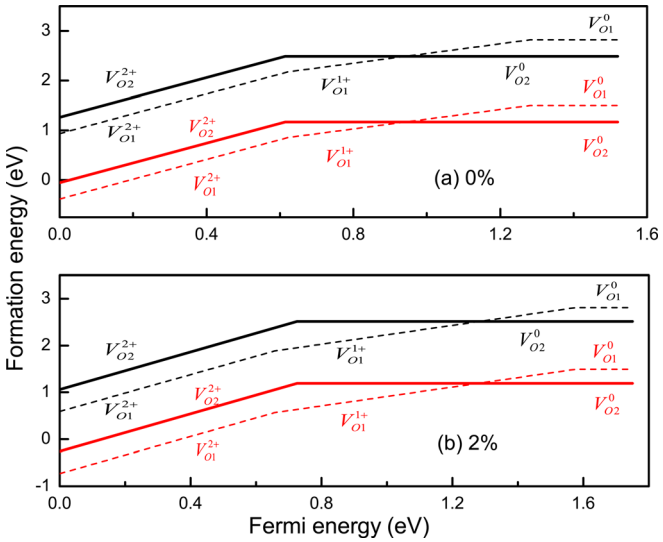

FIG. 4. (Color online) Formation energy of O vacancy with respect to the Fermi energy for (a) without strain condition and (b) 2% strain condition. The O chemical potential regions are varied within oxygen poor condition ($\Delta\mu_O = -1.319$ eV, lower lines/red) to oxygen rich condition ($\Delta\mu_O = 0$, upper lines/black). Only the formation energies of the stable charge state of O vacancy at corresponding Fermi level are shown. The Fermi level shifts from VBM, set to zero here, to the CBM of $BiCoO_3$ with corresponding strain.

Fig. 4(a)). As the tensile strain increases, the formation energy of charged defects decreases clearly, with a reduction of about 0.6 and 1.0 eV under 2% and 4% strains (plot for 4% is not shown in Fig. 4), respectively. Though there is no remarkable changes for the neutral vacancy defects, the formation of charged oxygen vacancies becomes easier as the strain increases.

C. Oxygen vacancy effect in $BiCoO_3$

From Sec. III B, we learned that the stable O vacancies in $BiCoO_3$ could be V_{O1}^{1+}, V_{O1}^{2+}, or V_{O2}^{0}, depending on the Fermi level. In the pure $BiCoO_3$, the bonding of Co–O1 shows a strong local interaction along the ⟨001⟩ direction with the bond length of 1.78 Å. The local magnetic moments at Co and O1 are found to be 2.85 μ_B and 0.36 μ_B, respectively. In contrast, the O2 ions usually hold no remnant magnetic moment, due to the symmetry of surrounding AFM Co ions in the xy plane. Consequently, O2 vacancies introduce no remnant magnetic moments, while vacancies V_{O1}^{1+} and V_{O1}^{2+} in $BiCoO_3$ introduce ordered spin charge and some remnant magnetic moments, as shown in Fig. 5. The oxygen vacancy–induced small peaks in the bandgap indicate that localized defect states are introduced in $BiCoO_3$ (c.f. Fig. 6). In comparison with V_{O1}^{2+}, more charges are accumulated in the Co-V_O-Co region near the valence band maximum (VBM) along ⟨001⟩ in the V_{O1}^{1+} case (not shown here). This also confirms that the transition level of 2+/1 + for O1 vacancy is located inside the bandgap; otherwise, the additional charge will be delocalized.

The total remnant magnetic moments introduced by V_{O1}^{1+} and V_{O1}^{2+} are 1 μ_B and 2.11 μ_B in the supercell, respectively. The integer value of remnant magnetic moment introduced by V_{O1}^{1+} indicates a half-metallic property of $BiCoO_3$ with V_{O1}^{1+} defects. The local magnetic moment of Co nearby the V_{O1}^{2+} defect is around 1.69 μ_B, in a clear contrast to the moment of other Co ions (2.85 μ_B), implying that the Co near the defect undergoes a significant electronic structure change. In fact, the charge within the Wigner-Seize radius is +0.771 e for the Co ion near the V_{O1}^{2+} defect, slightly greater than that of the Co ions away the defect (+1.031 e) or that of Co ions in the ideal lattice (+0.968 e). Obviously, the significant change of local magnetic moment for the Co ion near the V_{O1}^{2+} defect cannot be explained by the change of charges (or oxidation state).

To give a deeper insight of the electronic structure changes of Co ions introduced by oxygen vacancies, the decomposed projected density of states (PDOS) of 3d levels are plotted in Fig. 7 for Co ions in pure $BiCoO_3$ and nearby V_{O1}^{1+} and V_{O1}^{2+} defects. For Co in the pure $BiCoO_3$, it shows a d^6 configuration with the unoccupied spin down channels of e levels (d_{Z^2}, $d_{x^2-y^2}$) and d_{xz}, d_{yz}, in line with its oxidation state of 3+. In the decomposed PDOS of Co near the V_{O1}^{1+}, we noticed that the spin down channel of d_{Z^2} shifts lower in energy and is fully occupied, leading to a d^7 configuration. Thus, the local magnetic moment is reduced, but it contributes 1 μ_B net moment to the system. Interestingly, for Co nearby the V_{O1}^{2+} defect, the spin up channel of $d_{x^2-y^2}$ becomes unoccupied, while the spin down d_{Z^2} is fully occupied as it shifts much lower in energy. This clearly reduces the local magnetic moment of the Co ion and contributes a net

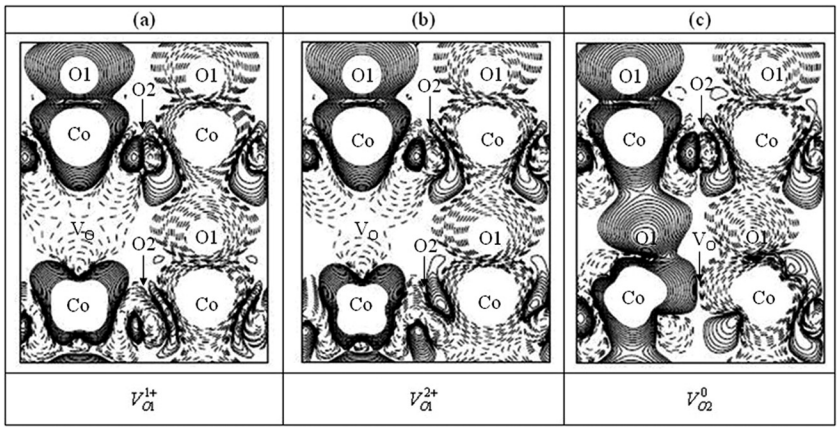

FIG. 5. Spin charge density of $BiCoO_3$ on (010) planes across the vacancy of (a) V_{O1}^{1+}, (b) V_{O1}^{2+}, and (c) V_{O2}^{0}, respectively. The spins up and down densities are denoted by solid and dashed lines, respectively. Here, the spin density contours start at 0.001 e/Å^3 and increases successively by a factor of $\sqrt{2}$.

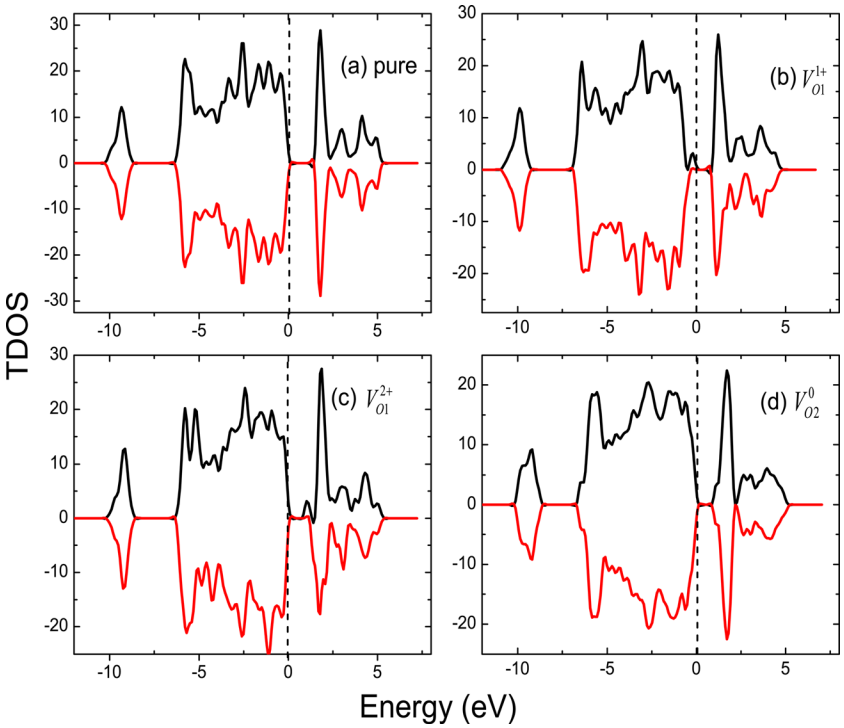

FIG. 6. (Color online) Total density of states (TDOS) of (a) pure $BiCoO_3$, (b) V_{O1}^{1+}, (c) V_{O1}^{2+}, and (d) V_{O2}^{0}.

magnetic moment of 2.11 μ_B to the system. Meanwhile, the new electronic distribution keeps a d^6 configuration for the Co and implies that the Co nearby the V_{O1}^{2+} defect keeps its oxidation state at 3+. It is known that, in an octahedral lattice, the e_g levels are higher than t_{2g} levels, due to the stronger overlap between the oxygen p orbitals and Co e_g orbitals. Here, the lower energy of d_{Z^2} levels of the Co nearby O1 vacancy should be attributed to the reduction of electron repulsion of d_{Z^2} levels as O1 is missing, which also significantly reduces the exchange splitting of d_{Z^2} (c.f. Fig. 7). The occupation of the decomposed 3*d* levels of various Co ions is also illustrated in Fig. 7.

The significant effect of O1 vacancy on the magnetic property of $BiCoO_3$ implies that O1 vacancy may provide an effective approach to tune the local magnetic moment of C-AFM $BiCoO_3$ and possibly introduce collective magnetic moments to the system. In contrast, the V_{O2}^{0} vacancy cannot change the total magnetic moment of the system, since the nearby AFM-coupled Co pair changes the same value of magnetic moment with opposite spin orientation, due to the formation of O2 vacancy.

When the tensile strain applies, V_{O1}^{1+}, V_{O1}^{2+}, and V_{O2}^{0} are still the most stable O vacancies in $BiCoO_3$ as the Fermi level shifts in the bandgap (c.f. Fig. 4). It is noticed that the

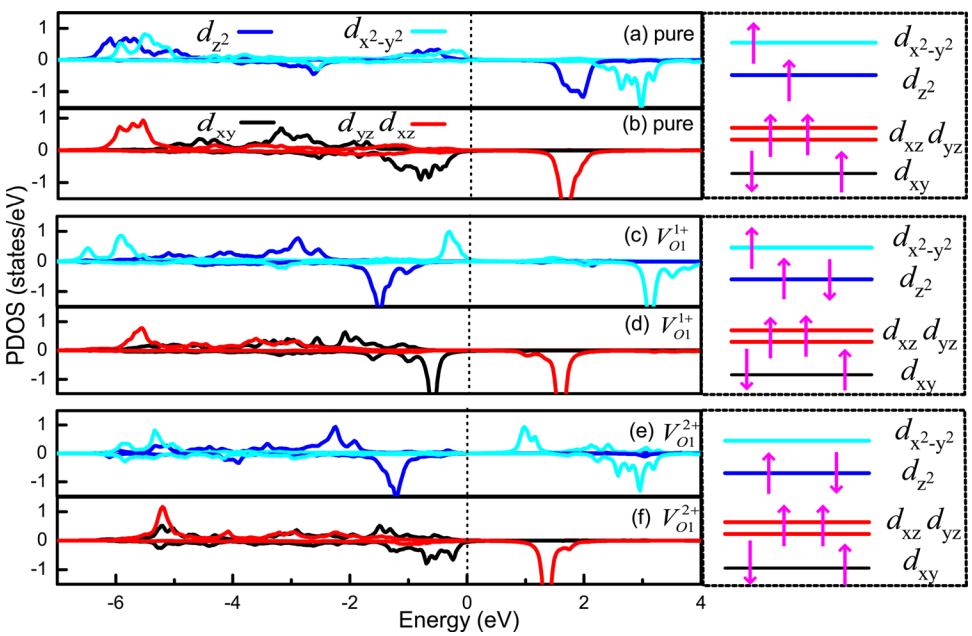

FIG. 7. (Color online) The decomposed DOS of Co *3d* levels in ideal $BiCoO_3$ [(a), (b)], nearby V_{O1}^{1+}[(c), (d)], and V_{O1}^{2+}[(e), (f)]. The occupation of the decomposed levels is also illustrated in the right side of the DOS. Here, the VBM is set to 0 and the spins up and down plots are denoted by positive and negative values, respectively.

TABLE II. The calculated polarization value along the ⟨001⟩ direction for pure $BiCoO_3$ and those with various O vacancies under situations of no strain and 2% strain.

		Pure	V_{O1}^{1+}	V_{O1}^{2+}	V_{O2}^{0}
P_s ($\mu C/cm^2$)	No strain	174.5	160.7	163.3	159.0
	2% strain	165.2	158.4	144.6	154.2

formation energy of the oxygen vacancies in the neutral charge state changes little, while that of positively charged defects decreases remarkably as the strain increases. This results in that the Fermi energy range for the stable V_{O2}^{0} vacancy becomes narrower as the strain increases, while the range for V_{O1}^{1+} vacancy expands. It is noted that the calculated bandgap of ideal $BiCoO_3$ is 1.52 eV, while its bandgap becomes about 1.70 eV with strains from 2%-4%. The V_{O1}^{1+} vacancy also captures an additional electron, which occupies the spin down d_{Z^2} of the nearby Co ion and shows 1 μ_B magnetic moment under strains up to 5%. Subsequently, the V_{O1}^{2+} vacancy shows similar magnetic property under strain. The Co ion (1.73 μ_B) nearby the O vacancy under 2% strain gets a critical magnetic moment change comparing with other Co ions (2.88 μ_B) and shows 2.24 μ_B total magnetic moment.

The influence of the oxygen vacancies on the ferroelectric polarization of $BiCoO_3$ was also studied. The values of ferroelectric polarization without strain and with 2% strain are collected in Table II. The tetragonal lattice was preserved for $BiCoO_3$ with oxygen vacancies in our calculations. The polarization along the xy plane was also calculated for $BiCoO_3$ with oxygen vacancies, since the symmetry restriction is removed by the vacancies. However, the calculated polarizations along the ⟨010⟩ and ⟨100⟩ directions turned out to be zero for the vacancied tetragonal $BiCoO_3$. Therefore, the polarization of $BiCoO_3$ with oxygen vacancy is along the ⟨001⟩ direction, as in the ideal $BiCoO_3$. The calculated results showed that the O vacancies slightly degrade the ferroelectric polarization, comparing with the pure $BiCoO_3$. The stable Co–O1 bond plays a critical role to maintain the ferroelectric property.[3] From Table III, the Co ion neighboring to the O1 vacancy shifts about 0.3 Å along the ⟨001⟩ direction toward the O2 plane due to the Coulomb attraction, leading to a lower polarization. In those of V_{O2}^{0} cases, the polarization values lower down by the reductive distance of between Bi and O1. In a word, the polarization values decrease slightly by oxygen vacancies.

TABLE III The relative atomic displacement along the ⟨001⟩ direction with respect to their ideal lattice sites in $BiCoO_3$ at no strain and 2% strain for Bi, Co, O1, and O2 near the vacancies. Positive and negative values stand for shifting up and down, respectively (c.f. Fig. 1).

		No strain			2% strain		
		V_{O1}^{1+}	V_{O1}^{2+}	V_{O2}^{0}	V_{O1}^{1+}	V_{O1}^{2+}	V_{O2}^{0}
Disp. (Å)	Bi	–0.009	0.030	–0.151	–0.008	0.040	–0.122
	Co	–0.262	–0.324	0.083	–0.310	–0.398	0.080
	O1	...	...	0.139	...	...	0.130
	O2	0.007	0.060	...	0.004	0.035	...

IV. CONCLUSION

In summary, we found that the polarization of $BiCoO_3$ decreases with the tensile strain, while the magnetic property is little affected by the tensile strain up to 5%. Following the investigation of the stable chemical potential range for $BiCoO_3$ and the formation energy of oxygen vacancies, we found that oxygen O1 vacancies with possible charge state of 1+ and 2+ could be formed, especially under oxygen poor condition, and the formation will be much easier as the tensile strain increases. It is interesting that the O1 vacancies will significantly change the local magnetic moment of Co ions and possibly provide collective magnetic moments to $BiCoO_3$, although the polarization of $BiCoO_3$ will be degraded slightly. The electronic structure and magnetic property of $BiCoO_3$ upon oxygen vacancy formation was also explained through the crystal field theory. As a result, the magnetic property and polarization of $BiCoO_3$ could be tuned by the oxygen vacancy and strain. This will enrich the physics of $BiCoO_3$ as a multiferroic material and broaden its possible application.

ACKNOWLEDGMENTS

We are grateful for the computer time at the High Performance Computer Center of Shenzhen Institute of Advanced Technology (SIAT), Chinese Academy of Science. This work was supported by NSFC (Grant No. 11174082), NCET-08-0202 and Education Foundation of Science and Technology Innovation of the Ministry of Education, China (Grant No. 708070).

[1]Y. Uratani, T. Shishidou, F. Ishii, and T. Oguchi, Jpn. J. Appl. Phys. **144**, 7130 (2005).
[2]A. A. Belik, S. Iikubo, K. Kodama, N. Igawa, S. Shamoto, S. Niitaka, M. Azuma, Y. Shimakawa, M. Takano, F. Izumi, and E. Takayama-Muromachi, Chem. Mater. **18**, 798 (2006).
[3]M. Q. Cai, J. C. Liu, G. W. Yang, Y. L. Cao, X. Tan, X. Y. Chen, Y. G. Wang, L. L. Wang, and W. Y. Hu, J. Chem. Phys. **126**, 154708 (2007).
[4]P. Ravindran, R. Vidya, O. Eriksson, and H. Fjellvag, Adv. Mater. **20**, 1353 (2008).
[5]X. Ming, X. Meng, F. Hu, C.-Z. Wang, Z.-F. Huang, H.-G. Fan, and G. Chen, J. Phys.: Condens. Matter **21**, 295902 (2009).
[6]Y. Uratani, T. Shishidou, and T. Oguchi, J. Phys. Soc. Jpn. **78**, 084709 (2009).
[7]K. Oka, M. Azuma, W. T. Chen, H. Yusa, A. A. Belik, E. Takayama-Muromachi, M. Mizumaki, N. Ishimatsu, N. Hiraoka, M. T. Sujimoto, M. G. Tucker, J. P. Attfield, and Y. Shimakawa, J. Am. Chem. Soc. **132**, 9438 (2010).
[8]X. Y. Chen, R. Y. Tian, J. M. Wu, Y. J. Zhao, H. C. Ding, and C. G. Duan, J. Phys.: Condens. Matter **23**, 326005 (2011).
[9]D. D. Cuong, B. Lee, K. M. Choi, H. S. Ahn, S. Han, and J. Lee, Phys. Rev. Lett. **98**, 115503 (2007).
[10]A. J. Hatt and N. A. Spaldin, Eur. Phys. J. B **71**, 435 (2009).
[11]J. H. Lee and K. M. Rabe, Phys. Rev. Lett. **104**, 207204 (2010).
[12]C. Ederer and N. A. Spaldin, Phys. Rev. B **71**, 224103 (2005).
[13]J. F. Ihlefeld, N. J. Podraza, Z. K. Liu, R. C. Rai, X. Xu, T. Heeg, Y. B. Chen, J. Li, R. W. Collins, J. L. Musfeldt, X. Q. Pan, J. Schubert, R. Ramesh, and D. G. Schlom, Appl. Phys. Lett. **92**, 142908 (2008).
[14]S. Ju and T. Y. Cai, Appl. Phys. Lett. **95**, 231906 (2009).
[15]J. G. Wu, G. Q. Kang, and J. Wang, Appl. Phys. Lett. **95**, 192901 (2009).
[16]Z. Zhang, P. Wu, L. Chen, and J. L. Wang, Appl. Phys. Lett. **96**, 232906 (2010).
[17]A. J. Hatt, N. A. Spaldin, and C. Ederer, Phys. Rev. B **81**, 054109 (2010).

[18]I. C. Infante, S. Lisenkov, B. Dupe, M. Bibes, S. Fusil, E. Jacquet, G. Geneste, S. Petit, A. Courtial, J. Juraszek, L. Bellaiche, A. Barthelemy, and B. Dkhil, Phys. Rev. Lett. **105**, 057601 (2010).
[19]D. G. Schlom, L. Q. Chen, C. B. Eom, K. M. Rabe, S. K. Streiffer, and J. M. Triscone, Annu. Rev. Mater. Res. **37**, 589 (2007).
[20]J. Wang, J. B. Neaton, H. Zheng, V. Nagarajan, S. B. Ogale, B. Liu, D. Viehland, V. Vaithyanathan, D. G. Schlom, U. V. Waghmare, N. A. Spaldin, K. M. Rabe, M. Wuttig, and R. Ramesh, Science **299**, 1719 (2003).
[21]G. Kresse and J. Furthmuller, Comput. Mater. Sci. **6**, 15 (1996).
[22]G. Kresse and D. Joubert, Phys. Rev. B **59**, 1758 (1999).
[23]J. P. Perdew and W. Yue, Phys. Rev. B **33**, 8800 (1986).
[24]J. P. Perdew and Y. Wang, Phys. Rev. B **45**, 13244 (1992).
[25]A. I. Liechtenstein, V. I. Anisimov, and J. Zaanen, Phys. Rev. B **52**, R5467 (1995).
[26]H. J. Monkhorst and J. D. Pack, Phys. Rev. B **13**, 5188 (1976).
[27]G. Makov and M. C. Payne, Phys. Rev. B **51**, 4014 (1995).
[28]R. D. King-Smith and D. Vanderbilt, Phys. Rev. B **47**, 1651 (1993).
[29]S. Picozzi and C. Ederer, J. Phys.: Condens. Matter **21**, 303201 (2009).
[30]H. Bea, M. Bibes, A. Barthelemy, K. Bouzehouane, E. Jacquet, A. Khodan, J. P. Contour, S. Fusil, F. Wyczisk, A. Forget, D. Lebeugle, D. Colson, and M. Viret, Appl. Phys. Lett. **87**, 072508 (2005).
[31]L. W. Martin, Q. Zhan, Y. Suzuki, R. Ramesh, M. F. Chi, N. Browning, T. Mizoguchi, and J. Kreisel, Appl. Phys. Lett. **90**, 062903 (2007).
[32]R. Wordenweber, E. Hollmann, R. Kutzner, and J. Schubert, J. Appl. Phys. **102**, 044119 (2007).
[33]C. Himcinschi, I. Vrejoiu, M. Friedrich, E. Nikulina, L. Ding, C. Cobet, N. Esser, M. Alexe, D. Rafaja, D. R. T. Zahn, J. Appl. Phys. **107**, 123524 (2010).
[34]R. Pick, M. H. Cohen, and R. M. Martin, Phys. Rev. B **1**, 910 (1970).
[35]D. Huang, Y.-J. Zhao, D.-H. Chen, and Y.-Z. Shao, Appl. Phys. Lett. **92**, 182509 (2008).
[36]S. J. Clark and J. Robertson, Appl. Phys. Lett. **94**, 022902 (2009).
[37]S. B. Zhang and J. E. Northrup, Phys. Rev. Lett. **67**, 2339 (1991).